

Modified LPE technique growth and properties of long wavelength $\text{InAs}_{0.05}\text{Sb}_{0.95}$ thick film

S.H. Hu, H.Y. Deng, Y. Sun, J. Wu, L.Y. Shang, T. Lin, R. Wang, N. Dai*

National Laboratory for Infrared Physics, Shanghai Institute of Technical Physics, Chinese Academy of Sciences, Shanghai 200083, PR China

Received 15 October 2007; received in revised form 24 October 2007; accepted 24 October 2007
Available online 4 November 2007

Abstract

$\text{InAs}_{0.05}\text{Sb}_{0.95}$ thick film with thickness of about $120\ \mu\text{m}$ was grown by modified LPE technique on InAs substrate. The Fourier transform infrared (FTIR) transmission measurement revealed that the cutoff wavelength (defined at the mid-transmittance) is $12.5\ \mu\text{m}$ for $\text{InAs}_{0.05}\text{Sb}_{0.95}$ thick film. An electron mobility of $23,900\ \text{cm}^2/\text{Vs}$ with a carrier density of $2.37 \times 10^{16}\ \text{cm}^{-3}$ at 300 K has been achieved. The investigation of the lattice dynamics of $\text{InAs}_{0.05}\text{Sb}_{0.95}$ has been made by using Raman scattering. These results indicate its potential applications for infrared detectors in long wavelength range and high-speed electron devices.

© 2007 Elsevier B.V. All rights reserved.

Keywords: Semiconductors; Crystal growth; Optical properties

1. Introduction

Photodetectors operating in the $8\text{--}12\ \mu\text{m}$ wavelength range are of great importance for applications in infrared (IR) thermal imaging. $\text{InAs}_{1-x}\text{Sb}_x$ has the smallest band gap among all conventional III–V alloys [1–3], which has attracted extensive interest for long-wavelength ($8\text{--}12\ \mu\text{m}$) optoelectronic applications. In recent years, ternary $\text{InAs}_{1-x}\text{Sb}_x$ has shown its potential usefulness for $8\text{--}12\ \mu\text{m}$ room-temperature devices [4–6]. The $\text{InAs}_x\text{Sb}_{1-x}$ is also useful for high-speed electron devices because of its very high electron mobility. Many growth techniques such as molecular beam epitaxy (MBE) [7], metal-organic chemical vapor deposition (MOCVD) [8] and liquid phase epitaxy (LPE) [9] have been employed to grow $\text{InAs}_{1-x}\text{Sb}_x$ ternary layers.

In this letter, we successfully developed $\text{InAs}_{0.05}\text{Sb}_{0.95}$ thick film with thickness of about $120\ \mu\text{m}$ by the conventional LPE process with appropriate and simple modifications. One of the critical factors in the modified LPE system is that the clearance between the substrate surface and the top surface of the boat is in the range of $100\text{--}150\ \mu\text{m}$, which is far beyond that of the

conventional LPE technique. As a result, some melt remains on the surface of the substrate and cools slowly to form a single crystal epilayer. Usually, the epilayer with thickness more than $100\ \mu\text{m}$ is impossible to obtain by MOCVD and MBE. The $100\ \mu\text{m}$ thickness plays the important role in reducing the influence of mismatch between epilayer and the substrate, which is advantaged for the highly lattice-mismatched heteroepitaxy. Moreover, thick ($>50\ \mu\text{m}$), low-defect, compositionally graded epitaxial layers of ternary and quaternary alloys, termed “virtual substrate” by Mao and Krier [10,11], would effectively satisfy many of the same functions of substrate wafers cut from ternary ingots. The growth of $\text{InAs}_x\text{Sb}_{1-x}$ by conventional LPE has so far been achieved only for low Sb composition (corresponding to $3\text{--}5\ \mu\text{m}$ gap) and for thin films with thickness of several micrometers [7–9]. This letter reported the investigation on the properties of $\text{InAs}_{0.05}\text{Sb}_{0.95}$ thick film grown by the modified LPE technique. As an important narrow band gap material, the optical and electric properties of $\text{InAs}_{0.05}\text{Sb}_{0.95}$ thick films are of both technical and scientific interest.

2. Experiments

The modified LPE growth was carried out in a conventional horizontal graphite sliding-boat system with an ambient of flowing Pd-membrane purified hydrogen at atmospheric pressure in a quartz reactor tube. The starting materials were 6N pure In and Sb, and undoped (non-doped) InAs. The substrates

* Corresponding author.

E-mail address: ndai@mail.sitp.ac.cn (N. Dai).

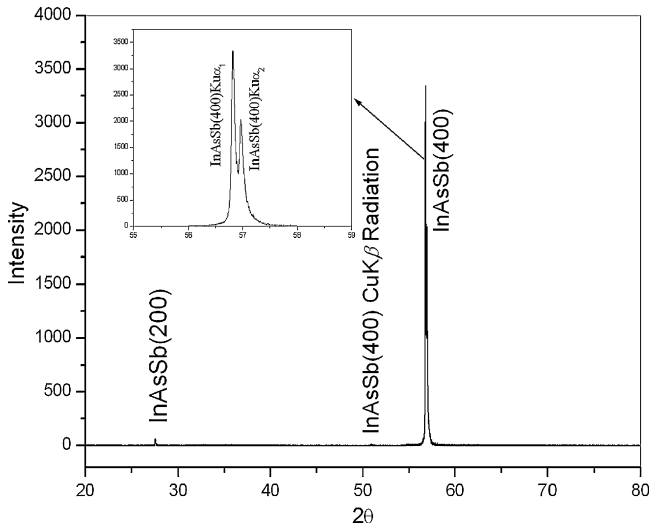


Fig. 1. XRD patterns of the $\text{InAs}_{0.05}\text{Sb}_{0.95}$ epilayer.

used were well-polished (100) InAs wafers, which was rinsed in acetone and ethanol by a supersonic cleaner, and chemically etched using mixture solution of H_2O_2 and HNO_3 (6:4) before setting into the growth system. Prior to growth, metals were baked out for 1 h at a temperature of 650°C in flowing hydrogen to remove residual impurities and reduce oxides. Next, the growth process began with an appropriate starting temperature (about 600°C for $\text{InAs}_{0.05}\text{Sb}_{0.95}$) and was ramped down with the certain cooling rate of $10^\circ\text{C}/\text{min}$. The quality of the epilayer is closely related to the starting growth temperature and the cooling rate.

3. Results and discussion

The X-ray diffraction measurement was carried out along the (400) plane of $\text{InAs}_{0.05}\text{Sb}_{0.95}/\text{InAs}$ samples. The main peak at a diffraction angle of 56.80° in Fig. 1 is from $\text{InAs}_{0.05}\text{Sb}_{0.95}$ epilayer. The sharpness of the main peak as seen in Fig. 1 indicates the high quality of the grown layer. The value of the full-width at half-maximum (FWHM = 324 arcsec) for (400) plane is comparable to that of InAs epilayer on GaAs substrate (FWHM = 320) by molecular beam epitaxy [12].

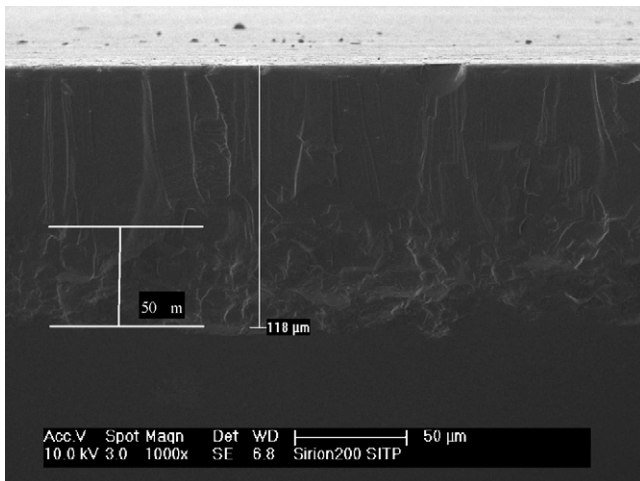


Fig. 2. SEM image of the cross-sectional view.

Fig. 2 presents the SEM images of the cross-sectional view. The cross-section image of a typical sample indicates a sharp interface between the InAsSb film and InAs substrate. The film exhibits a dense microstructure with no crack and voids. The thickness of the InAsSb epilayer is estimated to be about $120\ \mu\text{m}$. It is seen from Fig. 2 that a transition boundary region between the grown layer and the InAs substrate is as thick as about $50\ \mu\text{m}$, the orientation of the crystal in this interface layer is anomalous and full of misfit dislocation due to the large lattice mismatch. However, the rest of epilayer (about $60\ \mu\text{m}$) over the boundary area has rather good crystal perfection, as seen in Fig. 2.

The Fourier transform infrared (FTIR) transmission spectrum of $\text{InAs}_{0.05}\text{Sb}_{0.95}$ film at RT was obtained and is shown in Fig. 3. The wavelength at mid-transmittance of the absorption edge was defined as the cutoff wavelength. The cutoff wavelength in Fig. 3 reaches $12.5\ \mu\text{m}$, comparable to that of $\text{InAs}_{0.04}\text{Sb}_{0.96}$ epilayer by ME [13,14]. It is evident that the cutoff wavelength of $\text{InAs}_{0.05}\text{Sb}_{0.95}$ layer is shifted to longer wavelengths in comparison to $\text{InAs}_{0.06}\text{Sb}_{0.94}/\text{GaAs}$ [9], InSb/GaAs [15] and bulk InSb [16].

Raman scattering experiment was performed in a backscattering geometry and Raman spectra were excited by the 488 nm line of an Ar-ion laser. The laser output power was fixed at approximately 500 mW and was focused onto the sample using a cylindrical lens. The scattered light was collected with the sample surface parallel to the input slits of a Spex 1403 triple monochromator with a resolution of $2\ \text{cm}^{-1}$ and was detected with a GaAs photomultiplier equipped with photon counting electronics.

InSb and InAsSb have been amply probed by Raman methods [17–21]. Here we show the Raman scattering data of $\text{InAs}_{0.05}\text{Sb}_{0.95}$ film with high Sb composition and with thickness up to $120\ \mu\text{m}$. Fig. 4 shows the typical Raman spectra for the $\text{InAs}_{0.05}\text{Sb}_{0.95}$ film. The scattering range was from 100 to $300\ \text{cm}^{-1}$, which covers the frequencies of the optical-phonon modes of interest: InSb longitudinal-optical (LO) mode at

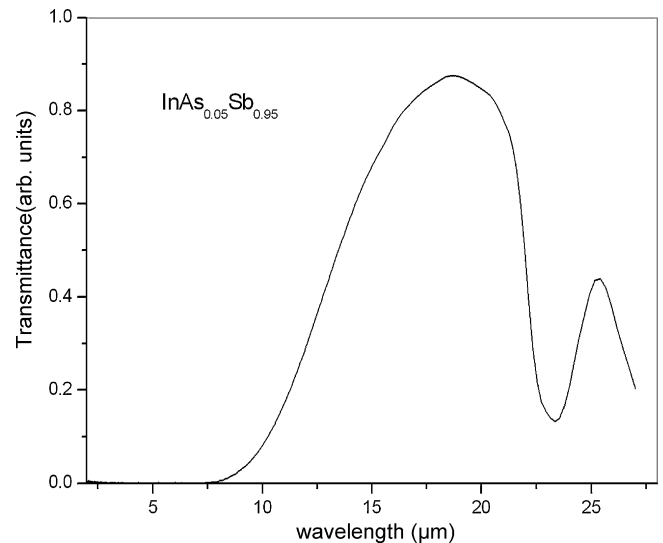


Fig. 3. Fourier transform infrared (FTIR) transmission spectrum.

Table 1
Electrical parameters of InAs_{0.05}Sb_{0.95} epilayer grown by modified LPE technique

Temperature (K)	Mobility (cm ² /V s)	Concentration (cm ⁻³)	Resistivity (Ω cm)	Hall coefficient (cm ³ /C)
300	23,900	2.37 × 10 ¹⁶	0.011	263

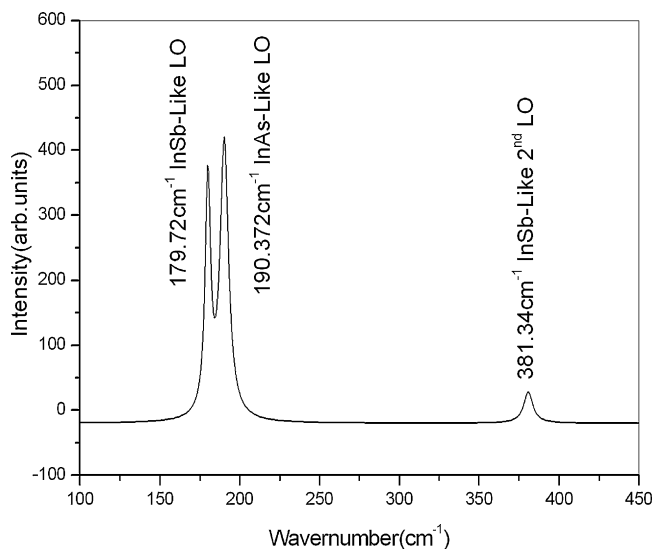


Fig. 4. Raman scattering measurement of InAs_{0.05}Sb_{0.95}/InAs at 300 K. Model 179.72 cm⁻¹ is assigned as InSb-like LO, 190.37 cm⁻¹ for InAs-like LO and 381.34 cm⁻¹ for InSb-like second LO.

193 cm⁻¹, InSb transverse-optical (TO) at 185 cm⁻¹, InAs LO mode at 242 cm⁻¹ and InAs TO mode at 220 cm⁻¹. The TO mode is forbidden for our scattering geometry. The narrow peak at 179 and 190 cm⁻¹ are the first order InSb-like and InAs-like LO phonon modes of InAs_{0.05}Sb_{0.95}, respectively. The weak peak at 386 cm⁻¹ is the second-order InSb-like LO phonon. The full widths at half maximum (FWHM) of the LO lines are 4.0 and 6.0 cm⁻¹ for the InSb-like and the InAs-like LO phonons, respectively. These linewidth values are comparable to those observed from epitaxial InSb films grown by metal-organic magnetron sputtering [22]. The small value of FWHM shows good crystallinity despite the large lattice mismatch (6%) in lattice constant between InAs_{0.05}Sb_{0.95} epilayer and InAs substrate.

The lattice dynamics in III–V ternary alloy systems display some interesting feature. For mixed crystals which shows “one-mode” behavior, such as GaInP [18]. Other ternary alloys, such as AlGaAs, GaAsP and GaPSb [19], show “two-mode” behavior, where two sets of optical phonons are observed over the entire range of alloy composition. The optical phonons of ternary compound InAs_xSb_{1-x} show a one + two-mode behavior, similar to the GaInAs and GaInSb systems [20]. InAs_{1-x}Sb_x alloy shows a one-mode behavior for the optical phonons in the composition range 0 < x < 0.6 and two-mode behavior for large value of x (x > 0.6) [21]. The lattice dynamics study by Raman scattering suggests two-mode behavior of the optical phonons for InAs_{0.05}Sb_{0.95} crystal grown by modified LPE techniques.

We measured the carrier concentration and electron mobility using van der Pauw measurement at 300 K for the InAs_{0.05}Sb_{0.95} epilayers. Prior to the measurements, the InAs substrates were

removed by grinding, in order to eliminate the influence from n-InAs substrate. Indium was used as the Ohmic contact. Hall coefficient indicates that the epilayers were n-type at 300 K. It is well known that the antimony is very easy to be volatilized during the epitaxial growth at about 600 °C due to its high vapor pressure, which results in antimony vacancy in InAsSb epilayers. In our InAs_{0.05}Sb_{0.95} sample, the antimony vacancy donors may be the origin of the n-type unintentionally doped epilayer. Table 1 lists measured electrical parameters of the InAs_{0.05}Sb_{0.95} epilayer at room temperature. The electron mobility of the InAsSb sample is 2.39 × 10⁴ cm²/V s, comparable to the mobility reported for InSb/GaAs samples grown by MBE and MOCVD [23–25]. The better transport properties are expected by removing the transition boundary region between the grown layer and the InAs substrate in followed research works.

4. Conclusion

In summary, InAs_{0.05}Sb_{0.95} film with thickness of about 120 μm was successfully developed by modified LPE techniques. The Fourier transform infrared (FTIR) transmission measurement revealed that the cutoff wavelength (defined at the mid-transmittance) is 12.5 μm. The lattice dynamics study by Raman scattering suggests two-mode behavior of the optical phonons for InAs_{0.05}Sb_{0.95} crystal. An electron mobility of 23,900 cm²/V s with a carrier density of 2.37 × 10¹⁶ cm⁻³ at room temperature was obtained by van der Pauw measurements, indicating the high quality of the epilayer.

Acknowledgements

The authors gratefully acknowledge the support of the National Nature Science Foundation (Grant No. 60708019). The authors would like to acknowledge the support of the Shanghai-Applied Materials Research and Development Fund (No. 06SA05) and Shanghai City Committee of Science and Technology, China (No. 06XD14020).

References

- [1] M. Razeghi, Eur. Phys. J. AP. 23 (2003) 149–205.
- [2] C. Peng, N.F. Chen, F. Gao, X.W. Zhang, C.L. Chen, J.L. Wu, Y. Yu, Appl. Phys. Lett. 88 (2006) 242108-1–242108-3.
- [3] S. Nakamura, P. Jayavel, T. Koyama, M. Kumagawa, Y. Hayakawa, J. Cryst. Growth 280 (2005) 26–31.
- [4] A. Rakovska, V. Berger, X. Marcadet, B. Vinter, G. Glastre, T. Oksenhendler, D. Kaplan, Appl. Phys. Lett. 77 (2000) 397–399.
- [5] M. Carras, J.L. Reverchon, G. Marrer, C. Renard, B. Vinter, X. Marcadet, V. Berger, Appl. Phys. Lett. 87 (2005) 102103-1–102103-2.
- [6] H. Ait-Kaci, J. Nieto, J.B. Rodriguez, P. Grech, F. Chevrier, A. Salesse, A. Joulle, P. Christol, Phys. Status Solidi (a) 202 (2005) 647–651.

- [7] X. Marcadet, A. Rakovska, I. Prevot, G. Glastre, B. Vinter, V. Berger, J. Cryst. Growth 227–228 (2001) 609–613.
- [8] J.D. Kim, D. Wu, J. Wojkowski, J. Piotrowski, J. Xu, M. Razeghi, Appl. Phys. Lett. 68 (1996) 99–101.
- [9] V.K. Dixit, B. Bansal, V. Venkataraman, H.L. Bhat, K.S. Chandrasekharan, B.M. Arora, J. Appl. Phys. 96 (2004) 4989–4997.
- [10] M.G. Mauk, A.N. Tata, J.A. Cox, J. Cryst. Growth 225 (2001) 236–243.
- [11] Y. Mao, A. Krier, Mater. Res. Soc. Symp. Proc. 450 (1997) 49–54.
- [12] Z.L. Miao, S.J. Chua, S. Tripathy, C.K. Chia, Y.H. Chye, P. Chen, J. Cryst. Growth 268 (2004) 18–23.
- [13] Y.Z. Gao, X.Y. Gong, H.F. Kan, M. Aoyama, T. Yamaguchi, Jpn. J. Appl. Phys. 38 (1999) 1939–1940.
- [14] Y.Z. Gao, X.Y. Gong, H. Kan, M. Aoyama, T. Yamaguchi, Jpn. J. Appl. Phys. 42 (2003) 4203–4206.
- [15] V.K. Dixit, B.V. Rodrigues, H.L. Bhat, R. Venkataraghavan, K.S. Chandrasekharan, B.M. Arora, J. Cryst. Growth 235 (2002) 154–160.
- [16] P. Mohan, N. Senguttuvan, S. Moorthy Babu, P. Santharaghavan, P. Ramasamy, J. Cryst. Growth 200 (1999) 96–100.
- [17] V. Senthilkumar, M. Thamilselvan, K. PremNazeer, Sa.K. Narayandass, D. Mangalaraj, B. Karunakaran, K.G. Kim, J.S. Yi, Vacuum 79 (2005) 163–170.
- [18] P. Galtier, J. Chevallier, M. Zigone, G. Martinez, Phys. Rev. B 30 (1984) 726–733.
- [19] Y.T. Cheng, M.J. Jou, H.R. Jen, G.B. Stringfellow, J. Appl. Phys. 63 (1988) 5444–5446.
- [20] S. Yamazaki, A. Ushirokawa, T. Katoda, J. Appl. Phys. 51 (1980) 3722–3729.
- [21] Y.T. Cherng, K.Y. Ma, G.B. Stringfellow, Appl. Phys. Lett. 53 (1988) 886–887.
- [22] Z.C. Feng, S. Perkowitz, T.S. Rao, J.B. Webb, J. Appl. Phys. 68 (1990) 5363–5365.
- [23] P.E. Thompson, J.L. Davis, J. Waterman, R.J. Wagner, D. Gammon, D.K. Gaskill, R. Stahlbush, J. Appl. Phys. 69 (1991) 7166–7172.
- [24] E. Michel, J.D. Kim, S. Javadpour, J. Xu, I. Ferguson, M. Razeghi, Appl. Phys. Lett. 69 (1996) 215–217.
- [25] J. Heremans, D.L. Partin, D.T. Morelli, C.M. Thrush, G. Karczewski, J.K. Furdyna, J. Appl. Phys. 74 (1993) 1793–1798.